Analytica Chimica Acta 730 (2012) 49–59

Contents lists available at SciVerse ScienceDirect

Analytica Chimica Acta

journal homepage: www.elsevier.com/locate/aca

Cytochrome c biosensor for determination of trace levels of cyanide and arsenic compounds

Xolile Fuku, Faiza Iftikar, Euodia Hess, Emmanuel Iwuoha, Priscilla Baker*

SensorLab, Department of Chemistry, University of the Western Cape, Private Bag X17, Bellville 7535, South Africa

ARTICLE INFO

Article history:
Received 12 October 2011
Received in revised form 1 February 2012
Accepted 3 February 2012
Available online 6 March 2012

Keywords:
Toxicity
Cytochrome c (cyt c)
Boron doped diamond (BDD)
Diffusion coefficients

ABSTRACT

An electrochemical method based on a cytochrome c biosensor was developed, for the detection of selected arsenic and cyanide compounds. Boron doped diamond (BDD) electrode was used as a transducer, onto which cytochrome c was immobilised and used for direct determination of Prussian blue, potassium cyanide and arsenic trioxide. The sensitivity as calculated from cyclic voltammetry (CV) and square wave voltammetry (SWV), for each analyte in phosphate buffer (pH = 7) was found to be in the range of $(1.1–4.5) \times 10^{-8}$ A μM^{-1} and the detection limits ranged from 4.3 to 9.1 μM. The biosensor is therefore able to measure significantly lower than current Environmental Protection Agency (EPA) and World Health Organisation (WHO) guidelines, for these types of analytes. The protein binding was monitored as a decrease in biosensor peak currents by SWV and as an increase in biosensor charge transfer resistance by electrochemical impedance spectroscopy (EIS). EIS provided evidence that the electrocatalytic advantage of BDD electrode was not lost upon immobilisation of cytochrome c. The interfacial kinetics of the biosensor was modelled as equivalent electrical circuit based on electrochemical impedance spectroscopy data. UV–vis spectroscopy was used to confirm the binding of the protein in solution by monitoring the intensity of the soret bands and the Q bands. FTIR was used to characterise the protein in the immobilised state and to confirm that the protein was not denatured upon binding to the pre-treated bare BDD electrode. SNFTIR of cyt c immobilised at platinum electrode, was used to study the effect of oxidation state on the surface bond vibrations. The spherical morphology of the immobilised protein, which is typical of native cytochrome c, was observed using scanning electron microscopy (SEM) and confirmed the immobilisation of the cytochrome c without denaturisation.

1. Introduction

Cytochrome c (MW 12,400) is primarily known as an electron-carrying protein between cytochrome c reductase (Complex III) and cytochrome c oxidase (Complex IV) in the inner mitochondria [1]. If its function of shuttling electrons has been disrupted due to poisoning of toxic compounds such as arsenic and cyanide compounds, tissues and organs that mainly depend on aerobic respiration such as central nervous system, muscles, lungs, heart, etc. are affected and this will lead to death since ATP will not be produced. Arsenic and cyanide compounds can both have an acute and a chronic effects, depending on the level of exposure [2].

Analysis of cyanide and arsenic compounds is very important because these compounds are widespread in nature, i.e. food, pesticides, antimicrobial drugs and in industries. The detection of these compounds using electrochemical methods of analysis is a more attractive option because they are inexpensive, highly sensitive and have long-term reliability and reproducibility. The electrochemical detection of these compounds has been reported, using carbon, platinum, mercury and gold as working electrodes [3]. Nevertheless, the severe detection condition can damage the electrode and cause fluctuating background currents. Some researchers have reduced this problem by modifying the electrode, or using other electrochemical detection techniques such as pulse electrochemical detection. BDD can be used to eliminate this problem without any pre-treatment of the electrode because of the stable surface morphologies and the surface carbon terminated by hydrogen [4]. BDD electrode is better than glassy carbon (GC) electrode because of low and stable voltammetric background. Therefore, the signal to background ratios of analytes are enhanced in the voltammetric measurements and a wide working potential window in aqueous electrolyte solutions is obtained [5].

Glassy carbon electrode (GCE) has been widely used and also work on cytochrome c using boron doped diamond as a working electrode has been reported, Geng et al., used a novel sandwich structured SiO_2 gel/cytochrome c (cyt c)/SiO_2 gel which was designed and constructed on conductive boron-doped diamond (BDD) film substrate [6]. Su et al., using oxidized-modified

* Corresponding author. Tel.: +27 21 9593051; fax: +27 21 9593055.
E-mail addresses: pbaker@uwc.ac.za, 3056484@uwc.ac.za (P. Baker).

0003-2670/$ – see front matter © 2012 Elsevier B.V. All rights reserved.
doi:10.1016/j.aca.2012.02.025

electrode with silver coating at various stages of KCN treatment [7] and Chen et al., using a nitrite biosensor based on cyt c [8].

The aim of the work was to construct a BDD/cytochrome c biosensor that is sensitive enough to determine not only cyanide and arsenic compounds but all toxic compounds e.g. mercury compounds, lead compounds, etc. that are harmful to the environment. Investigation of cyt c interaction by electrochemical methods and spectroscopic methods were carried out.

2. Experimental procedures

2.1. Reagents and materials

Cytochrome c horse heart (Type I product no. 105201), arsenic trioxide (product no. 202673), Prussian blue (product no. 03899) and potassium cyanide (product no. 60178) were purchased from Sigma–Aldrich. Phosphate buffer solution (PBS), 0.1 M, pH 7.0 was prepared from anhydrous disodium hydrogen phosphate (Na_2HPO_4) and sodium dihydrogen phosphate (NaH_2PO_4). Deionized water (18.2 MΩ) purified by a milli-QTM system (Millipore) was used for aqueous solution preparations. Analytical grade argon (Afrox, South Africa) was used to degas the system. Sodium hydroxide (99.9%), hydrochloric acid (75%) and nitric acid (65%) used were also purchased from Sigma–Aldrich. These chemicals were of analytical grade.

2.2. Apparatus and electrode preparation

2.2.1. Apparatus

Electrochemical experiments were performed using BAS100W Bioanalytical System (Model No. 100B). The three-electrode electrochemical cell comprised a platinum wire counter electrode, a Ag/AgCl (3 M) electrode and BDD electrode was used as a reference (3 mm in thickness and 0.07 in diameter). Universal Pulse-EIS Voltammetry VoltaLab (Model No. PGZ2402 674R052 N006, Radiometer Analytical S.A, made in France), Fourier transform infrared spectroscopy (FTIR) experiments were performed on a Perkin Elmer spectrometer (Spectrum 100), subtractive normalised Fourier transform infrared spectroscopy (SNFTIR) experiments were performed on (Type MISE-PS/09/Vertex 80v, made in Germany) UV–vis spectra were measured using Nicolette Evolution 100 Spectrometer (Thermo Electron Corporation, UK) and pH meter.

2.2.2. Electrode preparation

BDD electrode was cleaned using pads and Al_2O_3 powder of different sizes (1 μm, 0.3 μm, and 0.05 μm). The electrode was rinsed with distilled water after cleaning it with Al_2O_3 powder of different micrometers.

2.2.3. Activation of BDD electrode

After the electrode was cleaned, it was activated using 1 M nitric acid and it was also cleaned with the acid by running 20 cyclic scans at potentials of −1500 to 1500 mV to remove any impurities. Cyclic voltammetry at a scan rate of 50 mV s^{-1} was used for activation of BDD electrode. The electrode was then rinsed with distilled water and dried with argon gas in preparation of incubating and drop coating of the electrode.

2.2.4. Electrochemical measurements

The electrodes used for the construction of the biosensor were, boron doped diamond (BDD) electrode which was used as the working electrode, reference electrode (3 M Ag/AgCl) and platinum wire which was our counter electrode.

Incubation method was used in the preparation of the biosensor, after cleaning the electrode. Boron doped diamond (3 mm) electrode was incubated for 4 hrs in 4.06×10^{-4} M cyt c after cleaning and activation. CV and SWV data was recorded to observe the effect of varying scan rate and concentration of analyte.

After preparation of the biosensor, the specific modified BDD electrode was transferred to a 3-mL electrochemical cell containing 0.1 M pH 7.0 PBS, before electrochemical measurements. CV and SWV analysis were carried out at scan rates of 5, 10, 15, 20, 25 and 30 mV s^{-1} at potentials of +600 to −600 mV. Concentration dependent for CV and SWV at bare BDD in PBS was done, by adding 0 μM, 2 μM, 4 μM, 6 μM and 8 μM of analytes (arsenic trioxide, potassium cyanide and Prussian blue) respectively. The scan rate dependent response to analyte concentration was observed as well.

In SNFTIR experiments platinum electrode was used as the working electrode for the immobilisation of cyt c instead of BDD electrode due to the highly specialised nature of the sample chamber, UV–vis spectroscopy was used to identify absorption peak for the protein and for monitoring the binding event between protein and different concentrations of analyte. FTIR was used for characterisation of the immobilised cyt c on BDD electrode.

2.3. Numerical evaluation of data

Equations used for mathematically derived parameters and statistical evaluation of results were primarily sourced from (Bard and Faulkner) [10].

Calculation of diffusion coefficient for CV (irreversible);

$$I_{pc} = (2.99 \times 10^5) n(\alpha n_a) A C D^{1/2} \nu^{1/2} \quad (1)$$

where I_{pc} is the cathodic peak current, n_a is the number of electrons involved in the charge transfer process, A is the surface area of the electrode, α is the charge transfer coefficient, C is the concentration of the solution and D is the diffusion coefficient.

Calculation of surface coverage for CV and SWV (irreversible);

$$\frac{I_{pc}}{\nu} = \frac{n^2 F^2 A \Gamma}{4RT} \quad (2)$$

This is the Laviron's equation, where I_{pc} is the cathodic peak current, n is the number of electrons moles, A is the surface area of the electrode, F the Faraday's constant, ν is the scan rate, R is the gas constant (8.314 J K^{-1} mol^{-1}) and Γ is the surface coverage and the surface coverage.

Calculation of diffusion coefficient for SWV;

$$\Delta I_p = \frac{nFAC_c D_c^{1/2}}{\pi^{1/2} t_p{}^{1/2} \Delta \Psi_p} \quad (3)$$

where I_p is the peak current, t_p is the pulse width, ψ_p is the dimensionless peak current, F is the Faradaic current, n is the number of electrons, C is the concentration of the solution and D is the diffusion coefficient. $\Delta\psi_p$ is the current without dimensions and depends on, n number of moles, E_P peak potential and E_S static potential. The values of ψ_p may be obtained from references or experimentally determined.

Calculation of rate constants for CV and SWV;

$$k_s(E_P) = 2.18 \left[\frac{D\alpha n F \nu}{RT}\right]^{1/2} \quad (4)$$

where k_s is the electron transfer rate constant, the sweep rate ν, D is the diffusion coefficient, F the Faraday's constant, α is the charge transfer coefficient and T is the temperature.

Statistical equations were used to determine the significance between the two sets of data obtained by CV and SWV, to evaluate how well the two methods were compared.

$$\text{(a)}F\text{-test}: \qquad F = \frac{S_1^2}{S_2^2} \quad (5)$$

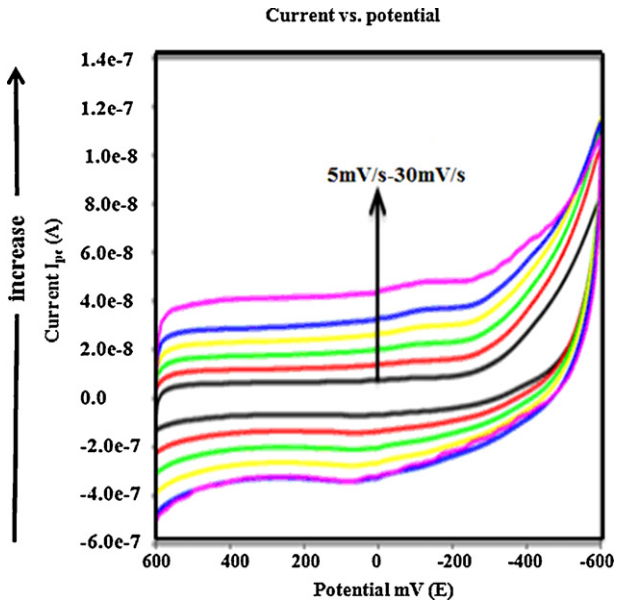

Fig. 1. CV for a bare BDD in PBS pH = 7 at different scan rates of 5, 10, 15, 20, 25 and 30 mV s^{-1}.

The *F*-test was used to determine the precision of the two methods. This test was used to compare means of CV and SWV data sets.

3. Results and discussion

3.1. Characterisation of BDD electrode in PBS

The electrochemistry of the bare BDD and the modified BDD (biosensor) electrode in 0.1 M PBS was investigated. CV of bare BDD in 0.1 M PBS (pH = 7) showed no distinguishable peaks (Fig. 1). However the biosensors displayed an irreversible reduction peak at −240 mV in 0.1 M PBS, pH = 7 (Fig. 2). Diffusion coefficient (D) and surface coverage (Γ) were calculated from plots of current vs. square root of scan rate from CV data and based on the slope of peak current vs. dimensionless peak current plot from SWV data (Figs. 3–5).

Dimensionless peak currents (ψ_p) were used for our calculation and the unknown values of ψ_p were determined experimentally. Reference values of ψ_p presented by Bard and Faulkner were also used. A graph of stepping potentials vs. dimensionless peak current was produced, from which the dimensionless currents ψ_p values for the scan rates used in our experiments were extrapolated.

Scan rate dependent cyclic voltammetry confirms a diffusion controlled system, evidenced by increasing peak current as a function of increasing scan rate (Fig. 3). The calculated diffusion

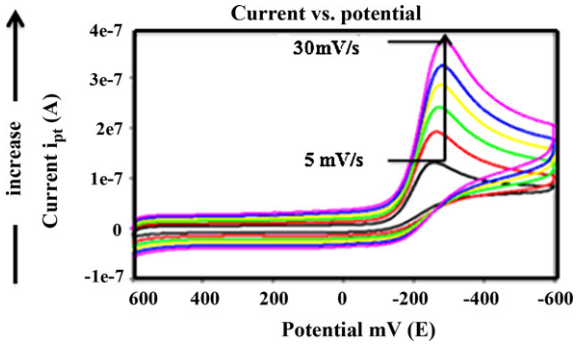

Fig. 2. CV for biosensor in 0.1 M PBS pH = 7 at different scan rates of 5, 10, 15, 20, 25 and 30 mV s^{-1}.

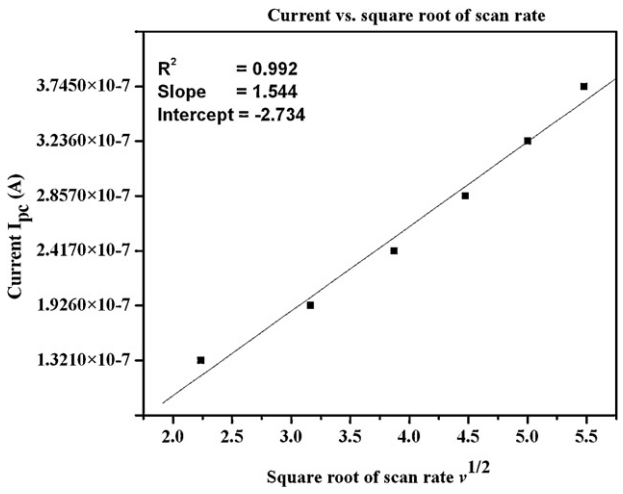

Fig. 3. Cytochrome c at various root scan rates for diffusion controlled system.

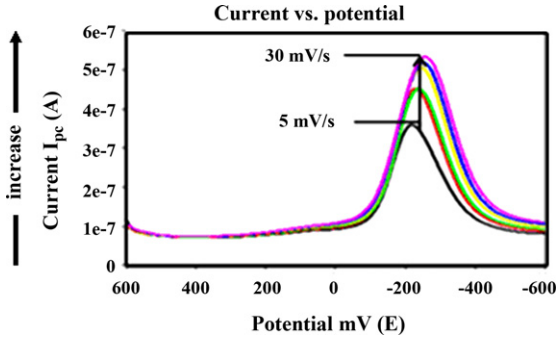

Fig. 4. SWV for biosensor in 0.1 M PBS pH = 7 at different scan rates of 5, 10, 15, 20, 25 and 30 mV s^{-1}.

coefficients for the biosensor, was found to be 5.09×10^{-10} cm^2 s^{-1} from CV data and 10.00×10^{-10} cm^2 s^{-1} using SWV data. The diffusion coefficient of SWV was observed to have higher value than CV, due to higher sensitivity of SWV technique (10^{-8}), however the values obtained are of the same order of magnitude.

The surface concentration of the biomolecule at the BDD electrode surface in PBS was calculated using Laviron's equation, and was found to be 1.7×10^{-12} mol cm^{-2}. This was similar to values obtained previously for monolayer coverage [7,8]. The k_s values were calculated to be 2.7×10^{-5} cm s^{-1} from data CV and to be

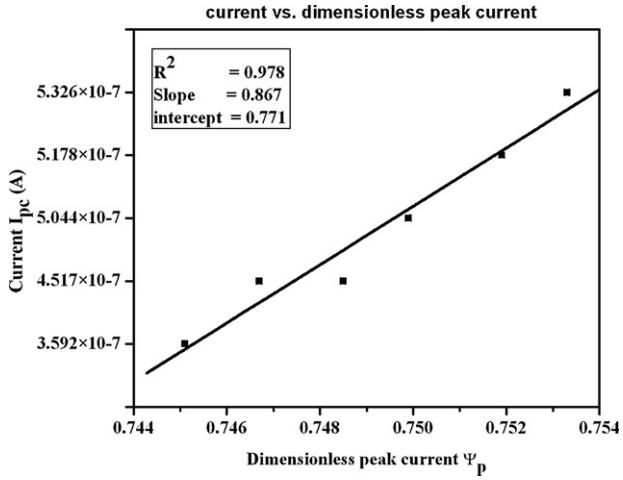

Fig. 5. SWV peak currents vs. dimensionless peak currents.

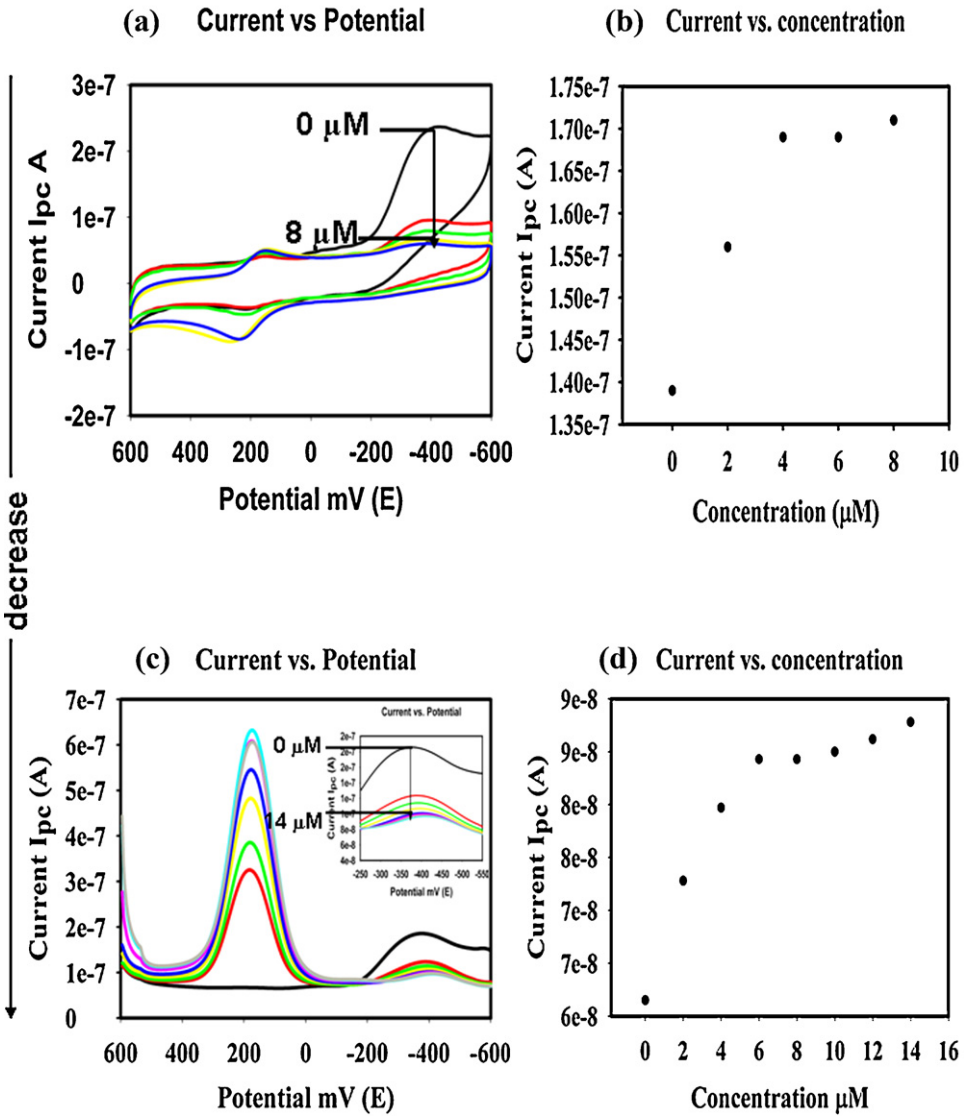

Fig. 6. (A) CV of biosensor in 0.1 M PBS (pH = 7) at 25 mV s^{-1} with Prussian blue (0, 2, 4, 6, 8 and 10 µM), (B) calibration curve for CV of biosensor in 0.1 M PBS pH = 7 at different concentrations of Prussian blue (0, 2, 4, 6, and 8 µM), (C) SWV of biosensor in 0.1 M PBS pH = 7 with Prussian blue (0, 2, 4, 6 and 8 µM) and (D) calibration curve for SWV of biosensor in 0.1 M PBS pH = 7 at different concentrations of Prussian blue (0, 2, 4, 6 and 8 µM).

5.3×10^{-5} cm s^{-1} from SWV data. The results obtained for the two systems by CV and SWV are in good agreement.

3.2. Biosensor response

Cytochrome c is thought to carry a net positive charge since the positive amino acids predominate [9]. In the construction of the biosensor in the current research, cyt c was used for the efficient quantitative measurement of some well known asphyxiants such as CN^-, As_2O_3 and $Fe_2K(CN)_{12}{\cdot}16H_2O$, through irreversible binding to the positive side chains on the protein surface. Scan rate and concentration dependence studies were carried out for biosensor response to Prussian blue ($Fe_2K(CN)_{12}{\cdot}16H_2O$), using CV and SWV. The biosensor response was also compared to the bare BDD electrode response to the Prussian blue.

3.3. Prussian blue (PB)

The diffusion coefficients of the biosensor were calculated using Eq. (1) for CV, was found to be 1.00×10^{-9} cm^2 s^{-1} for Prussian blue. This was smaller than literature value obtained by Liu et al., 5.90×10^{-7} cm^2 s^{-1}, using GCE/cyt c modified with 1-pyrenebutyric acid/MWNT, in 0.1 M PBS. The surface coverage was calculated using Eq. (2), was found to be 2.7×10^{-12} mol cm^{-2}. Geng et al., calculated a surface coverage of 2.2×10^{-9} mol cm^{-2}, using a nitrite biosensor based on cytochrome c. The theoretical value for monolayer coverage by Chen et al., was found to have same order of magnitude as the one we obtained 1.4×10^{-12} mol cm^{-2}. This places our value obtained for surface coverage well within the range of surface coverage obtained for various modified surfaces employing cyt c as biosensing element. The diffusion coefficient calculated from SWV was obtained using Eq. (3) for Prussian blue and was calculated to be 9.00×10^{-9} cm^2 s^{-1}.

A reversible peak for the oxidation–reduction of Fe^{3+}/Fe^{2+} was observed at formal potential of +198 mV in the presence of Prussian blue. The peak current for this couple increased with every additions of analyte (Prussian blue). Another irreversible peak was observed at reduction potential of −240 mV but shifted to more negative potentials and decreased with increasing concentration of the analyte. This peak was identified as the biosensor response peak, indicating binding between PB and immobilised protein. The calibration plots based on the reduction peak current vs.

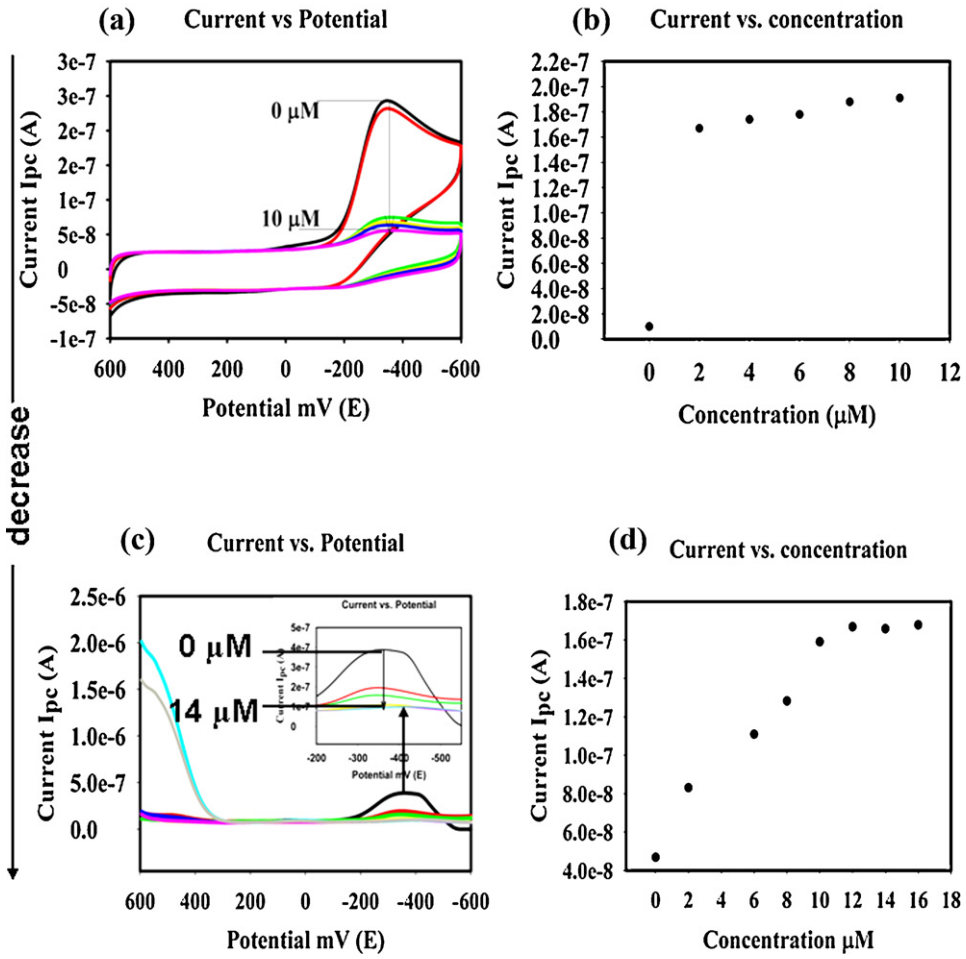

Fig. 7. (A) CV of biosensor 0.1 M PBS (pH = 7) at different concentrations of potassium cyanide (0, 2, 4, 6 and 8 µM), (B) calibration curve for KCN, (C) SWV of biosensor 0.1 M PBS (pH = 7) at different concentrations of potassium cyanide (0, 2, 4, 6 and 8 µM) and (D) calibration curve for KCN.

concentration was used to quantify the binding of Prussian blue. A decrease in peak currents was observed with each consecutive addition of analyte, indicating binding mechanism between analyte and biosensor (Fig. 6A–D).

Cyanide ligands on Prussian blue binds to the protein thus blocking the electron transfer of the protein resulting in a decrease in current with each addition of PB. The experiment also confirmed that the heme site of the protein was unaffected by cyanide binding to the immobilised protein. This is a significant result since it confirms a completely different interaction between PB (CN^- ligand) and cytochrome c as opposed to free CN^- and cytochrome c oxidase. Binding to the heme group is the mechanism responsible for most biosensors which are based on cytochrome c oxidase. The statistical analyses were carried out to determine the precision between the two methods i.e. CV and SWV using the same sample (Prussian blue). The standard deviation was found to be 1.36×10^{-8} for CV and 1.19×10^{-8} for SWV and the mean values for Prussian blue were calculated to be 1.61×10^{-7} for CV and 8.29×10^{-8} for SWV. In this case the *F*-test was used ($n = 6$) with $F_{crit} = 5.05$ at 95% confidence level, which was higher than the *F* values calculated 0.773. The null hypothesis was accepted and this confirms that the two methods are equivalent in precision and are comparable.

3.4. Potassium cyanide, KCN

The diffusion coefficients for KCN were calculated from CV and SWV using the irreversible Eq. (1) for CV and Eq. (2) for SWV and were found to be in good agreement i.e. 1.05×10^{-9} cm^2 s^{-1} for CV and 1.15×10^{-9} cm^2 s^{-1} for SWV. The rate constant was calculated using Eq. (4) and found to be 4.8×10^{-2} s^{-1} for CV and 6.1×10^{-3} s^{-1} for SWV. Compared to literature values from similar systems our rate constant values are one order of magnitude smaller i.e. 2.4 s^{-1} and 1.4 s^{-1} Koh et al., and the surface coverage calculated using Laviron's equation, was found to be1.4×10^{-11} mol cm^{-2}.

3.5. Arsenic trioxide, As_2O_3

The influence of the scan rate was investigated to determine whether the system was diffusion controlled or adsorption process. The diffusion coefficient obtained from CV was 2.00×10^{-9} cm^2 s^{-1} for arsenic trioxide. The surface coverage was calculated using Laviron's equation was found to be 3.1×10^{-12} mol cm^{-2} and that of potassium cyanide was calculated to be 1.4×10^{-11} mol cm^{-2}. Surface coverage in literature shows a wide degree of variability [6], however the values are in good agreement with theoretical value 1.4×10^{-12} mol cm^{-2} for monolayer coverage [8]. Diffusion coefficient from SWV for arsenic trioxide was found to be 9×10^{-9} cm^2 s^{-1}. The rate constants k_s were calculated as 1.067×10^{-4} s^{-1} (CV) and 1.229×10^{-9} s^{-1} (SWV), indicating facile electron transfer.

3.6. Biosensor response as a function of increasing concentration of potassium cyanide and arsenic trioxide

The biosensor response to As_2O_3 and KCN concentration shows a hyperbolic response, indicating no cooperative binding of the

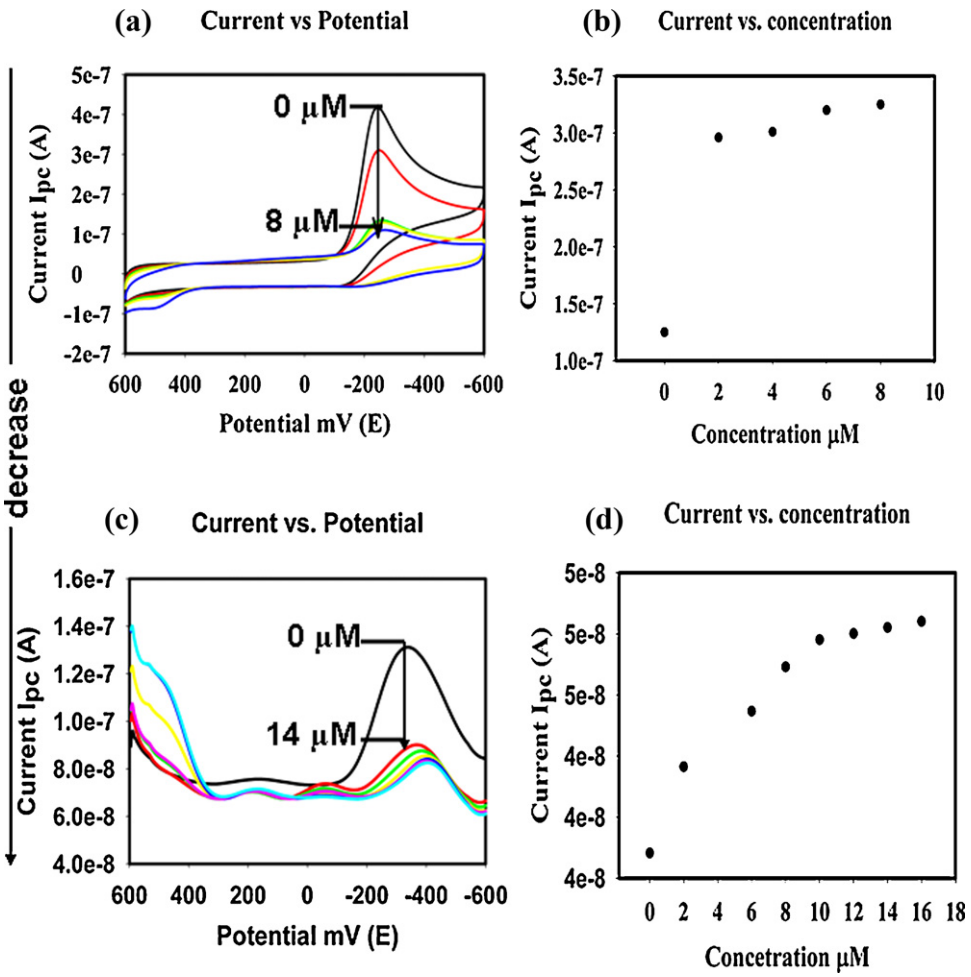

Fig. 8. (A) CV of biosensor in 0.1 M PBS (pH = 7) at different concentrations of arsenic trioxide (0, 2, 4, 6, 8 and 10 µM), (B) calibration curve for As_2O_3, (C) SWV of biosensor in 0.1 M PBS pH = 7 at different concentrations of arsenic trioxide (0, 2, 4, 6 and 8 µM) and (D) calibration curve for As_2O_3.

protein (Figs. 7B & D and 8B & D). The protein concentration is independent of the analyte molecule that binds to the active site/amino acids side chains of the protein. Cooperative binding would show sigmoidal/allosteric response between analyte and protein, because binding of analyte to one of the subunits or monomers alters affinity of other subunits for analyte. A sigmoidal shape of the binding curve would indicate that the analyte-binding sites of protein interact with each other such that the binding of one molecule of analyte to one protein facilitates binding of other analyte molecules to the other protein sites.

3.6.1. Detection limits and sensitivity for KCN and As_2O_3

The results show a decrease in current with an increase in concentration of arsenic trioxide and potassium cyanide, showing binding of potassium cyanide and arsenic trioxide to the protein cyt c by inhibiting the electron transfer therein (Figs. 7A & C and 8A & C and Table 1). The same decreasing trend was observed by Su et al., where the binding of KCN to the protein was studied. The magnitude of the reductive peak after addition of cyanide became smaller [7]. Figs. 7B & 8B for CV and Figs. 7D & 8D for SWV show the response of the biosensor to cyanide and arsenic compounds. The linear range which refers to the concentration range that can be determined with a linear calibration curve [21–23], was determined from our calibration curves for i.e. KCN, $Fe_2K(CN)_{12}{\cdot}16H_2O$ and As_2O_3 and were found to be 0–10 µM for KCN and As_2O_3 and 0–6 µM for $Fe_2K(CN)_{12}{\cdot}16H_2O$ (SWV).

The biosensor was able to measure far below the EPA and WHO guidelines (200 µg L^{-1} for cyanide and 10 µg L^{-1} for arsenic) [1–20] and the results of the two methods were statistically significant. The standard deviations of the detection limit for KCN was found to be 7.56×10^{-8} and 8.92×10^{-8} using CV and SWV data. The corresponding values for As_2O_3 were 6.85×10^{-8} and 5.39×10^{-8} from CV and SWV data. The mean values were found to be 2.75×10^{-7} and 1.22×10^{-7} for KCN and 1.54×10^{-7} and 1.12×10^{-7} for As_2O_3. The *F*-test performed on the standard deviation ($n = 6$), at 95% confidence level for diffusion coefficient data by CV and SWV, confirmed that the methods give equivalent precision and they are comparable at 95% confidence level.

Table 1
Calculated detection limit and sensitivity from CV and SWV for the analytes.

	Sensitivity (A µM^{-1})	Detection limit (µM)	Linear dynamic range (µM)
CV (KCN)	3.9×10^{-8}	4.22	0–2
CV (As)	2.1×10^{-8}	8.08	0–4
CV (PB)	1.8×10^{-8}	9.09	0–4
SWV (KCN)	4.5×10^{-8}	9.08	0–10
SWV (As)	1.9×10^{-8}	22.02	0–10
SWV (PB)	1.1×10^{-8}	37.49	0–6

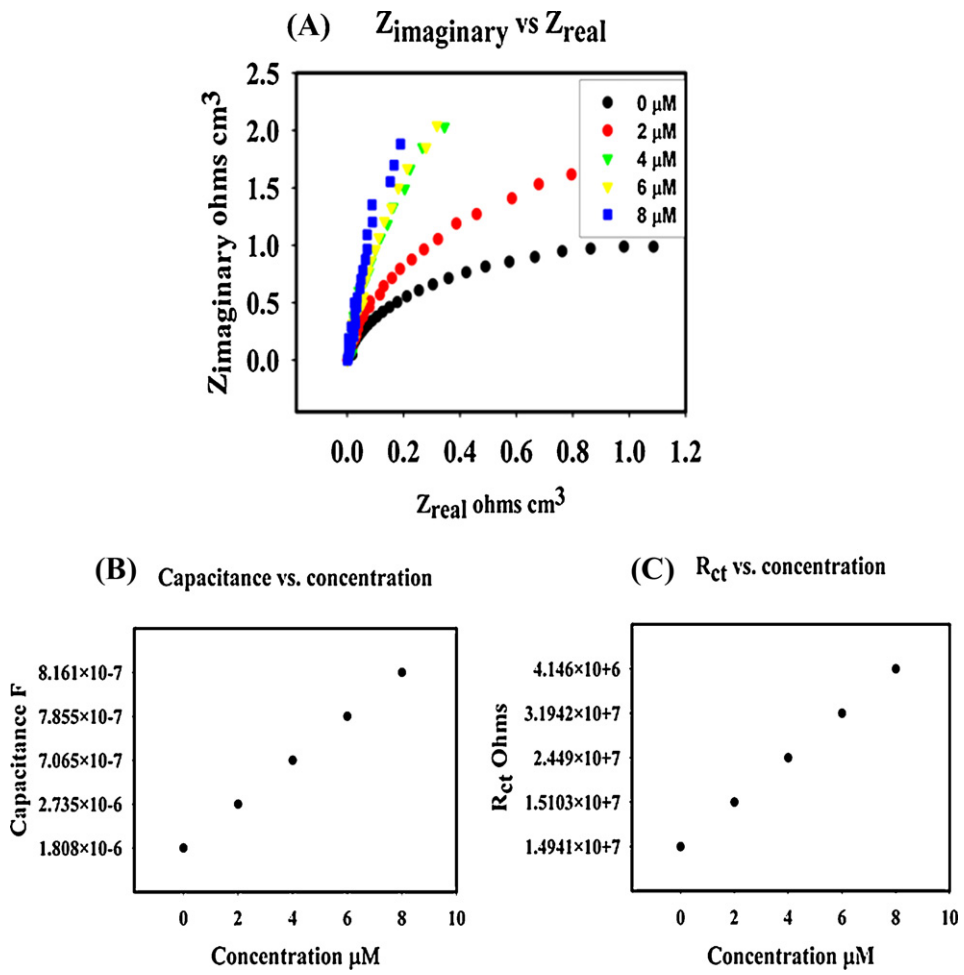

Fig. 9. (A) Nyquist plots of impedance for biosensor at different Prussian blue concentration, at potential of −300 mV (vs. Ag/AgCl), (B) calibration curve based on interfacial capacitance of biosensor response to Prussian blue and (C) calibration curve based on interfacial charge transfer resistance of biosensor response to Prussian blue.

3.7. Electrochemical impedance spectroscopy (EIS)

The potential controlled impedance behaviour of the biosensor was measured at potentials starting at −250 mV and stepped by 50 mV increments. The frequency range used was 1 kHz–100 mHz. A simple Randles circuit was used to model the biosensor (Fig. 12).

3.7.1. Biosensor response to analytes as measured by EIS

3.7.1.1. Prussian blue, $Fe_2K(CN)_{12}{\cdot}16H_2O$. Electrochemical impedance spectroscopy (EIS) can provide useful information on the impedance changes of the electrode surface during the fabrication process. The semicircle at higher frequencies corresponds to the electron-transfer-limited process and its diameter is equal to the electron transfer resistance (R_{et}), which controls the electron transfer kinetics of the redox probe at the electrode interface, while the linear region at lower frequencies corresponds to the diffusion process [10].

The impedance response of the biosensor to Prussian blue shows a gradual change in interfacial electrochemistry as a function of changing concentration (Fig. 9A). It is evident that the binding event takes place at concentrations higher than 2 µM. Modelling the data as an equivalent electrical circuit (Fig. 12) and plotting the interfacial capacitance and resistance as a function of concentration (Fig. 9B and C), provided numerical data that agrees well with the detection limit obtained by CV and SWV (Table 2).

Table 2
Calculated detection limit and sensitivity from EIS for the analytes.

	Sensitivity ($\Omega\,\mu M^{-1}$)	Detection limit (µM)
KCN	0.5	9.97
As	0.5	8.99
PB	0.5	9.00

3.7.1.2. Potassium cyanide, KCN. The binding of CN^- to the biosensor yields a marked change in the interfacial electrokinetics towards a system dominated by a capacitive interface (Fig. 10). This is characteristic of irreversible binding events, which facilitates the attachment of the analyte to the available biosensor surface. The extent of binding is governed by the availability of biomolecule and the size of the analyte molecule. Equivalent circuit fitting analysis supports the detection limits obtained by SWV analysis. Calibration curve confirmed the linear range determined by CV and SWV when monitoring the binding event in terms of interfacial capacitance or charge transfer resistance.

3.7.1.3. Arsenic trioxide, As_2O_3. It is evident from the complex plot of the biosensor response to As_2O_3 that there is a marked difference in the interfacial electrokinetics after the addition of more than 2 µM As_2O_3 as the impedance becomes more diffusional. This is in good agreement with the detection limit for the biosensor towards As_2O_3 as determined by CV i.e. 8.1 µM. The EIS method may not

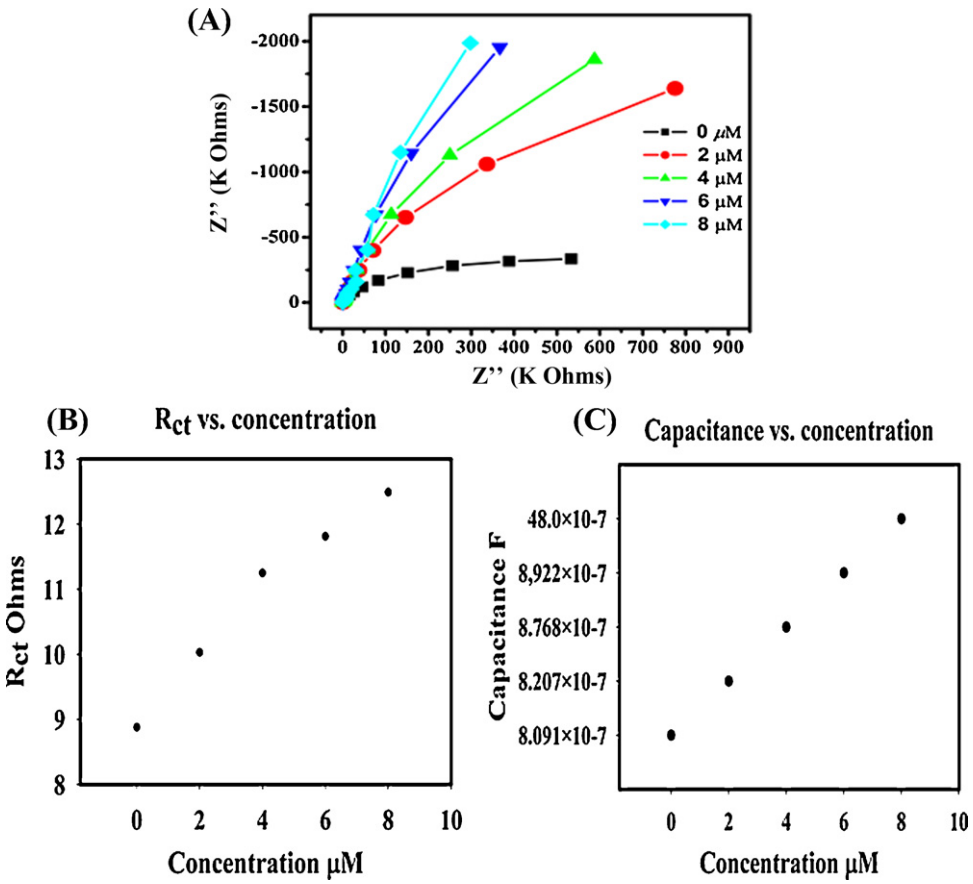

Fig. 10. (A) Nyquist plots of impedance for biosensor at different KCN concentration, at potential of −300 mV (vs. Ag/AgCl), (B) calibration curve based on interfacial charge transfer resistance biosensor response to KCN and (C) calibration curve based on interfacial capacitance of biosensor response to KCN.

lend itself as easily towards field measurements as CV or SWV, but could be a useful laboratory monitoring tool for fast and highly sensitive measurement of As_2O_3. The parameters (capacitance and charge transfer resistance) obtained from the Randles Sevcik circuit (Fig. 12) were used to construct calibration curves (Fig. 11B and C). Both parameters displayed a positive correlation with increasing analyte concentration, confirming the binding event.

As the concentration of analyte is increased the typical semi-circle nature of the system, which tells us about the electron transfer kinetics of the system, changed towards a more capacitive representation. This trend is due to an increase in the charge transfer resistance (R_{ct}) of the system as a function of increasing concentration. The electrochemical system becomes diffusion controlled at higher concentration. The electron transfer process at the interface is slowed down due to the increasing capacitive layer developing at the interface, when opposite charges bind due to electrostatic attraction.

Detection limits determined from CV and SWV calibration plots are in good agreement with the detection limits of EIS calibration plots (1 and 2).

3.8. UV–vis spectroscopy

The UV–vis analysis was carried out to confirm the binding of the analyte to the protein in solution. UV–vis analysis of a 0.1 M solution of cytochrome c prepared in phosphate buffer (pH = 7) was recorded for observation of cytochrome c before and after successive additions of the respective analyte.

Cytochrome c displayed two characteristic UV–vis absorption bands i.e. the soret band at 409 nm and the Q band at 550 nm (Fig. 13A). The band at 409 nm is the soret band and the one at 550 nm is the Q-band. According to literature [11] these bands are essentially π–π^* band associated with the porphyrin ring which is present in protein cyt c. The electronic absorption spectrum of a typical porphyrin ring consists of a strong transition to the second excited state (S0 → S2) at about 410 nm (the soret or B band) and a weak transition to the first excited state (S0 → S1) at about 550 nm (the Q band). The soret band is allowed and therefore intense. The Q band is forbidden, it is observed because of vibronic coupling with the soret band. Upon addition of different concentrations of arsenic trioxide, potassium cyanide and Prussian blue, respectively, a small decrease in the absorption intensity of the sorbet band and Q bands were observed, indicating that the environment of the protein had changed. A slight shift at 409–410 nm was observed also suggesting a change in the protein's structure. This was interpreted as evidence of analyte binding to the native cytochrome c in solution. A plot of absorbance vs. concentration showed a strong linear relationship for the binding event over the concentration range used and this linearity was confirmed by correlation coefficient of 0.99 in each case (Fig. 13B(i)–(iii)). The molar adsorption coefficient (ε) for cytochrome c was found to be 4.05 cm^{-1} mM^{-1} for potassium cyanide, 1.59 cm^{-1} mM^{-1} for arsenic trioxide and 2.43 cm^{-1} mM^{-1} for Prussian blue at 409 nm [12]. The rate of binding is proportional to molar adsorptivity, therefore the biosensor shows a higher affinity for potassium cyanide show compared to Prussian blue and arsenic trioxide. These ligands have their own metal centres which can facilitate electron transfer to metal centres on the ligands, therefore lowering the binding affinity.

Therefore UV–vis absorbance analysis was able to confirm the binding of the analyte to the cytochrome c in solution, since the

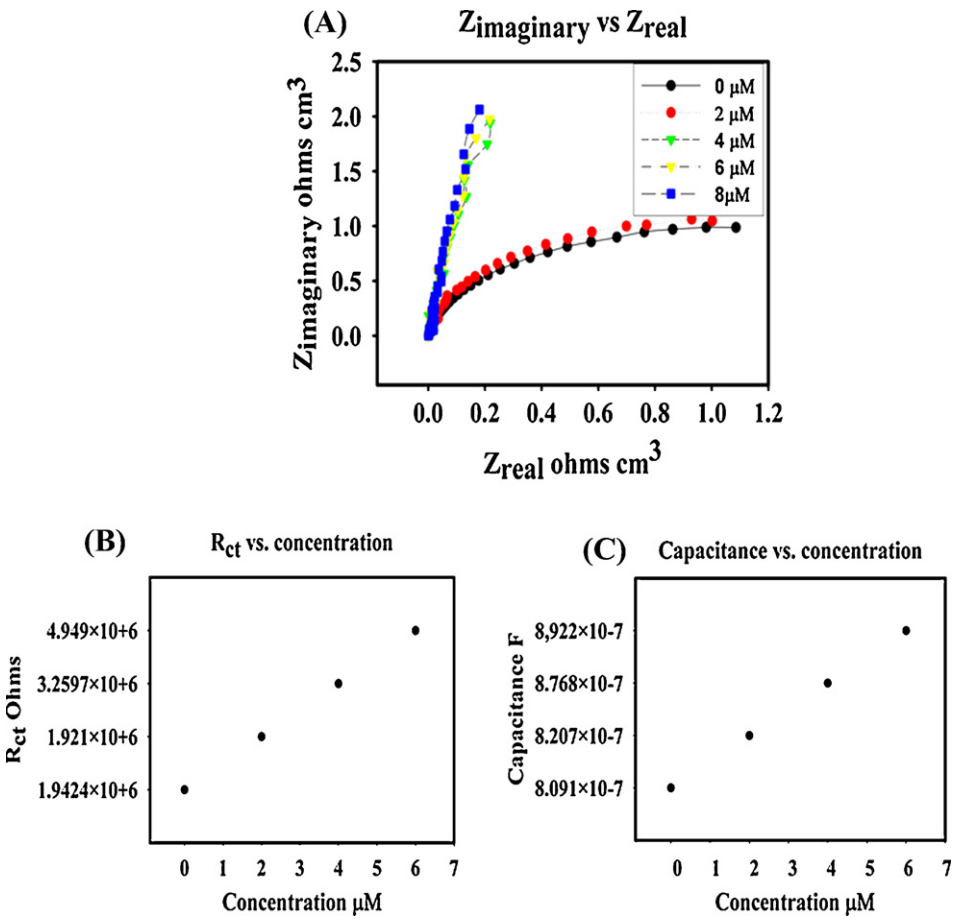

Fig. 11. (A) Nyquist plots of impedance for biosensor at different As_2O_3 concentration, at potential of −300 mV (vs. Ag/AgCl), (B) calibration curve based on interfacial capacitance of biosensor response to As_2O_3 and (C) calibration curve based on interfacial charge transfer resistance biosensor response to As_2O_3.

soret bands and Q bands are associated are considered to be purely electronic transitions involving the porphyrin ring of the heme [11]. This observation served to confirm the CV and SW data which indicated that the main interaction between the analyte and the cytochrome c was in fact not at the heme site but rather at the amino acids attached to the protein sites.

3.9. SNIFTIR results

Cytochrome c was drop coated onto a Pt disk electrode of diameter of 70 mm and interferograms were recorded using Ag/AgCl reference electrode and Pt wire counter electrode. Spectra were obtained at potentials from 0 mV to −700 mV at 100 mV intervals. Spectra were also recorded in the reverse direction. Spectra were obtained by Fourier transformation after averaging 300 interferograms acquired at each potential. The CaF_2 window was used in order to limit the influence of solvent on the spectra. Infrared spectra have been normalized with respect to the reference spectrum collected at −500 mV and are displayed as $\Delta R/R$ $[(R_s - R_r)/R_r]$ difference spectra. SNIFTIRS spectra obtained in this way therefore, contain only information of the molecular changes occurring from modification of the protein. Potentials of −200 mV, −300 mV and −400 mV were closely analysed, since our reductive peak potential in CV and SWV was observed in this region (Fig. 14).

The upward spectra show a decrease in absorption and downward show an increase in absorption spectra. The peak at 2081 cm^{-1} decreases in absorption intensity and develops a shoulder as the potential was stepped from −200 to −400 mV at 2081 cm^{-1}. A small doublet was observed at 2084 cm^{-1} which merged into a single peak and became more intense as we stepped through the reduction potentials. These vibrations were interpreted as evidence of the C—C and C=C resonance structures within the prophyrin rings which may develop potential induced alkyne resonance structures. The small peak observed at 2046 cm^{-1}, due to C—N stretching, was associated with an intermediate reduction state and disappeared at −400 mV. A doublet appears in SNFTIR spectra because of Fermi resonance, which may be observed in S—H and N—H functional group stretching. The shift in peak position and reduction of peak intensity as a function of stepped potential, was observed at 2010 cm^{-1} and was assigned to the C=N and C=C stretches, Cytochrome c (MW 12,400) consists of a single polypeptide chain of 104 amino acid residues and covalently attached to a heme group [13]. The heme is surrounded by many tightly packed hydrophobic side chains. Therefore we concluded that, the

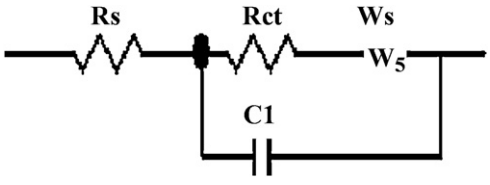

Fig. 12. Circuit used for all impedance analysis.

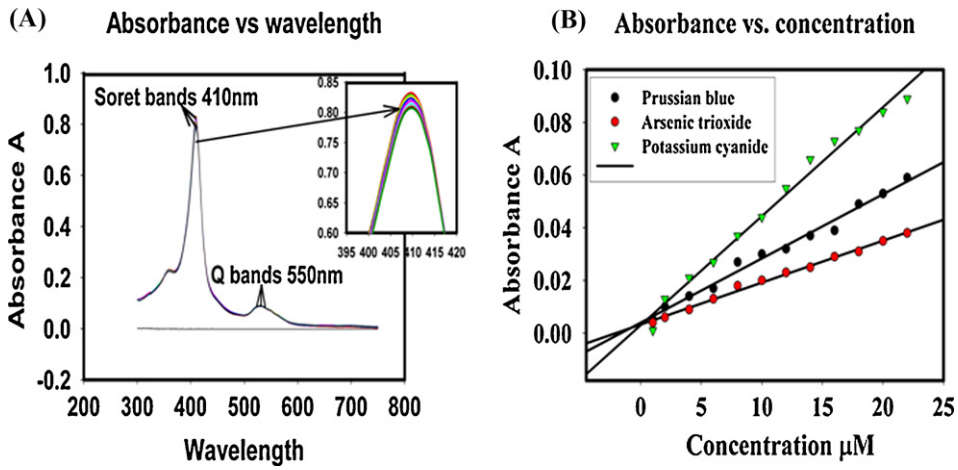

Fig. 13. (A) UV–vis absorption spectra for cytochrome c solution (pH = 7) with As_2O_3 concentration 2, 4, 6, 8, 10, 12, 14, 16, 18, 20, 22 and 24 μM and (B) (i) calibration curve for biosensor response to KCN concentration, (ii) calibration curve for biosensor response to As_2O_3 concentration and (iii) calibration curve for biosensor response Prussian blue to concentration.

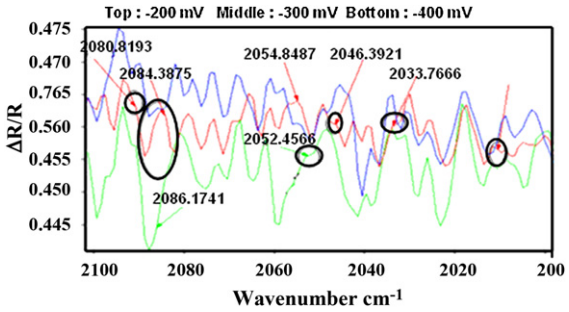

Fig. 14. SNIFTIRS spectra of Pt/cyt c showing the enlargement of the finger print region.

behaviour observed in SNIFTIR correlates well with infrared spectra of cytochrome c obtained in literature references for immobilised cyt c and confirmed the efficient adsorption of the protein onto the BDD electrode, in the biosensor assembly [14]. SNFTIR results confirm that the functional groups within the protein, undergoes many resonance vibrations. Resonance vibrations were associated with the porphyrin ring and amino acid side chains and did not indicate any permanently ruptured bonds, therefore supporting evidence from UV–vis spectroscopy, that the protein was not denatured in the immobilised state.

3.10. Scanning electron microscopy (SEM) for cyt c

A scanning electron microscope (SEM) images a sample by scanning it with a high-energy beam of electrons in a raster scan pattern. The electrons interact with the atoms that make up the sample producing signals that contain information about the sample's surface topography, composition, and other properties such as electrical conductivity. cyt c structural morphology has been studied using this technique (SEM). Fig. 15A shows SEM images of gold foils with dimensions of 12 cm^2 modified with HA (humic acid)–cyt c [15] and Fig. 15B shows SEM images for cyt c on gold screen printed electrode at 10 μm.

Cytochrome c is known to be roughly spherical in nature, with a diameter of 34 Å [1,16,17]. From our preparation we were able to observe dense spherical-shaped particles, distributed uniformly on the surface of the gold screen printed electrode. SEM images gave the direct visual evidence that cyt c is attached on the electrode surface. The spherical-shapes show native nature of the protein and shows that the protein still retains its stability and it is not denatured. The results are in good

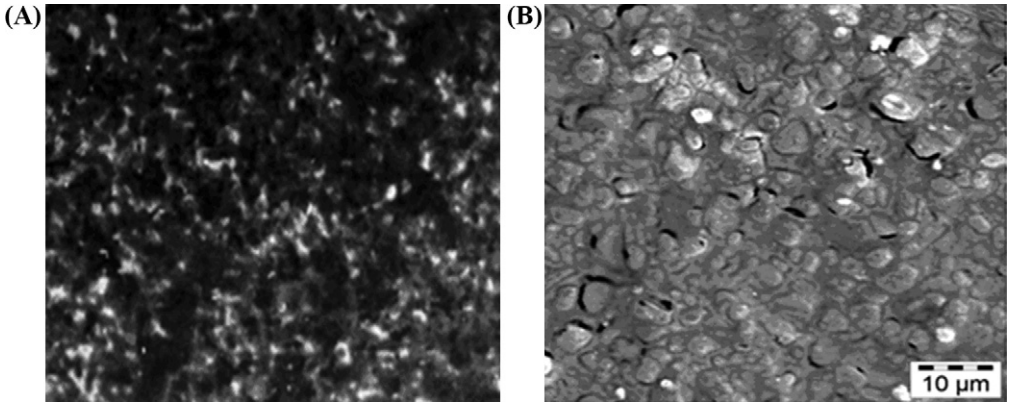

Fig. 15. (A) SEM images for HA–cyt c and (B) SEM images for cyt c.

agreement with the spherical shape of the protein from literature (Fig. 15A). This result has also been confirmed by UV–vis analysis where the stable peak of the protein was observed at 408 (soret bands). The protein peak slightly changed its shape upon addition of different concentrations of the analyte into the solution.

4. Conclusion

A biosensor, developed on an activated BDD platform by immobilisation of cytochrome c, was prepared in a simple and quick manner. CV and SWV confirmed the presence of an irreversible reduction peak at −240 mV which was used for monitoring the binding between the analytes and the biosensor. In this work the reduction peak observed at reduction peak potentials of −240 mV was an irreversible peak and was due to the protein (cytochrome c). Similar findings were also reported [18,19]. Based on these findings it is concluded that the irreversible reduction peak at negative potentials is not denatured but showed a change in protein structure. Interfacial kinetic parameters such as charge transfer resistance and capacitance, as measured by EIS, were quantitatively related to the concentration dependent binding of analyte to the biosensor. The biosensor was shown to have low detection limit ranging from 0.27–55 mg L^{-1} for the cyanide and 1.58–4.31 mg L^{-1} for arsenic compound compared to the world health organisation (WHO). The biosensor also showed low sensitivity for the analytes KCN, $Fe_2(CN)_{12}{\cdot}16H_2O$ and As_2O_3. The sensitivity and the detection limits of the biosensor were quantified using voltammetry (CV and SWV) as well as electrochemical impedance spectroscopy (EIS). The sensitivity and detection limit of the biosensor for these selected analytes (established to be in the micro molar range) were much lower than sensitivity and detection limit of other analytical methods (Groom and Luong) [20]. Square wave voltammetry and cyclic voltammetry show a linear response to the selected analytes. EIS confirmed linear response of biosensor below 10 μM to these analytes (KCN, As_2O_3 and $Fe_2(CN)_{12}{\cdot}16H_2O$) when binding event was measured as capacitance or resistance.

UV–vis absorption spectroscopy was used to confirm the binding of the individual analyte compounds to the native protein in solution, by measuring the response of the soret band at 409 nm as a function of concentration. The molar adsorptivity coefficient for the protein binding was determined as 2.43 cm mM^{-1} (PB), 4.05 cm mM^{-1} (KCN) and 1.59 cm mM^{-1} (As_2O_3). Biosensor showed the highest affinity for KCN as evidenced by molar adsorptivity coefficient. Prussian blue which also contains CN^-, the proposed binding site was observed to have lower molar adsorptivity coefficient. This may be due to steric factors associated with the structure of $Fe_2(CN)_{12}{\cdot}16H_2O$. As_2O_3 was observed to have the lowest molar adsorptivity coefficient of the analytes investigated. Binding affinity may also be reduced by electron delocalisation onto metal centres in these two ligands. Spectroscopic techniques (SNFTIR, and FTIR) were used to confirm the native state of the immobilised cytochrome c on BDD, Au and Pt electrodes. FTIR confirmed the bond vibrations of the surface functional groups associated with the protein amino acid backbone and SNFTIR showed the resonance coupling of these functional groups as the protein is electrochemically reduced.

Acknowledgments

We acknowledge financial support from National Research Foundation (NRF) South Africa and Organization for the Prohibition of Chemical Weapons (OPCW).

References

[1] H. Senn, K. Wüthrich, Amino acid sequence, haem–iron co-ordination geometry and functional properties of mitochondrial and bacterial c-type cytochromes, Quarterly Reviews of Biophysics 18 (1985) 111–134.
[2] U.N. Dwivedi, P. Singh, V.P. Pandey, A. Kumar, Structure–function relationship among bacterial, fungal and plant laccases, Journal of Molecular Catalysis B: Enzymatic 68 (2011) 117–128.
[3] G.M. Whitesides, J. Yang, R. Ferrigno, Xiaoxi Chen, Redox properties of cytochrome c adsorbed on self-assembled monolayers: a probe for protein conformation and orientation, American Chemical Society 18 (2002) 7009–7015.
[4] S. Girotti, E.N. Ferri, M.G. Fumo, E. Maiolini, Monitoring of environmental pollutants by bioluminescent bacteria, Analytica Chimica Acta 608 (2008) 2–29.
[5] Y. Zhou, J. Zhi, The application of boron-doped diamond electrodes in amperometric biosensors, Talanta 79 (2009) 1189–1196.
[6] R. Geng, G. Zhao, M. Liu, M. Li, A sandwich structured SiO_2/cytochrome c/SiO_2 on a boron-doped diamond film electrode as an electrochemical nitrite biosensor, Biomaterials 29 (2008) 2794–2801.
[7] L. Su, J.B. Kelly, F.M. Hawkridge, M.C. Rhoten, S.I. Baskin, Characterization of cyanide binding to cytochrome c oxidase immobilized in electrode-supported lipid bilayer membranes, Journal of Electroanalytical Chemistry 581 (2005) 241–248.
[8] Q. Chen, S. Ai, X. Zhu, H. Yin, Q. Ma, Y. Qiu, A nitrite biosensor based on the immobilization of Cytochrome c on multi-walled carbon nanotubes–PAMAM–chitosan nanocomposite modified glass carbon electrode, Biosensors and Bioelectronics 24 (2009) 2991–2996.
[9] B. Ge, F. Lisdat, Superoxide sensor based on cytochrome c immobilized on mixed-thiol SAM with a new calibration method, Analytica Chimica Acta 454 (2002) 53–64.
[10] A.J.L.R.F. Bard, Electrochemical Methods: Fundamentals and Applications, 2nd ed., 2000, pp. 854–879.
[11] S.E.W.-W. Stefan Franzen, A.P. Shreve, Heme charge-transfer band III is vibronically coupled to the soret band, American Chemical Society 124 (2002) 7148.
[12] G. Battistuzzi, M. Borsari, J.A. Cowan, A. Ranieri, M. Sola, Spectroelectrochemical determination of the redox potential of cytochrome c via multiple regression, Chemical Society 83 (2002) 5315–5324.
[13] Cytochrome c gene and protein expression: developmental regulation, environmental response, and pesticide sensitivity in *Aedes aegypti*, Journal of Medical Entomology 45 (2008) 401–408.
[14] B.W.D.a.K.D., Absorption spectra and some other properties of cytochrome c and of its compounds with ligands, Royal Society 156 (1962) 429–458.
[15] J.-J. Xu, G. Wang, Q. Zhang, D.-M. Zhou, H.-Y. Chen, Interfacing cytochrome c to Au electrodes with humic acid film, Electrochemistry Communications 6 (2004) 278–283.
[16] C. Xiang, Y. Zou, L.-X. Sun, F. Xu, Direct electron transfer of cytochrome c and its biosensor based on gold nanoparticles/room temperature ionic liquid/carbon nanotubes composite film, Electrochemistry Communications 10 (2008) 38–41.
[17] P.C.A. Marken, F.D. Asogan, Direct cytochrome c electrochemistry at boron-doped diamond electrodes, Electrochemistry Communications 4 (2002) 62–66.
[18] G.-C. Zhao, Z.-Z. Yin, L. Zhang, X.-W. Wei, Direct electrochemistry of cytochrome c on a multi-walled carbon nanotubes modified electrode and its electrocatalytic activity for the reduction of H_2O_2, Electrochemistry Communications 7 (2005) 256–260.
[19] N.K. Sagara, T. Sone, A. Hinnen, C. NikiK, Redox reaction mechanism of cytochrome c at modified gold electrodes, American Chemical Society 6 (1990) 254–262.
[20] J.H.T. Luong, C. Masson, R.S. Brown, K.B. Male, A.L. Nguyen, Monitoring the activity of glucose oxidase during the cultivation of Aspergillus niger using novel amperometric sensor with 1,1′-dimethylferricinium as a mediator, Biosensors and Bioelectronics 9 (1994) 577–584.
[21] D.A. Skoog, D.M. West, Fundamentals of Analytical Chemistry, 8th ed., 2004, p. 215.
[22] J. McNally, The Importance of Linear Dynamic Range for Small Molecule and Targeted Peptide LC–MS/MS Quantitation, Thermo Fisher Scientific, San Jose, CA, USA, 2011.
[23] D.W. Koppenaal, The importance of linear dynamic range for small molecule and targeted peptide LC–MS/MS quantitation, in: Analytical Chemistry, 2005, p. 419a.